

Biphoton compression in standard optical fiber: exact numerical calculation

G. Brida,¹ M. V. Chekhova,^{2,1} I. P. Degiovanni,¹ M. Genovese,¹ G. Kh. Kitaeva,² A. Meda,¹ and O. A. Shumilkina²

¹*Istituto Nazionale di Ricerca Metrologica, Strada delle Cacce 91, 10135 Torino, Italy*

²*Department of Physics, M.V.Lomonosov Moscow State University,
Leninskie Gory, 119991 Moscow, Russia*

(Dated: August 14, 2018)

Generation of two-photon wavepackets, produced by spontaneous parametric down conversion in crystals with linearly chirped quasi-phase matching grating, is analyzed. Although being spectrally broad, two-photon wavepackets produced this way are not Fourier transform limited. In the paper we discuss the temporal compression of the wavepackets, exploiting the insertion of a standard optical fiber in the path of one of the two photons. The effect is analyzed by means of full numerical calculation and the exact dispersion dependencies in both the crystal and the fiber are considered. The study opens the way to the practical realization of this idea.

PACS numbers: Valid PACS appear here

I. INTRODUCTION

One of the problems in modern quantum optics is generation of two-photon light with given spectral and temporal properties. In particular, of considerable interest is preparation of two-photon wavepackets with small correlation times. Studies in this direction are important, first of all, from the viewpoint of the fundamental question: how well can we localize a photon of a correlated pair if its twin is registered at a certain time? Furthermore, two-photon wavepackets with small correlation times are required for quantum technology applications involving interactions between matter and nonclassical light [1–5], as well as for quantum metrology applications [6]. Several ideas have been suggested for generating two-photon states with broad spectra, all based on Spontaneous Parametric Down Conversion (SPDC). Among them, one can mention prisms or diffraction gratings introducing a frequency chirp [7], SPDC in aperiodically poled crystals (APPC) [8–10] or in crystals with temperature gradients [11]. However, a broad spectrum of two-photon light does not necessarily lead to small correlation times, although the inverse is true [12–14]. Similarly, in classical optics, a broadband pulse is not always short in time, although the spectrum of a short pulse is always broad. Indeed, the spectrum broadening introduced in Refs. [7, 10, 11] is inhomogeneous, in the sense that two-photon wavepackets generated in different parts of the crystal have different spectra. As a result, the two-photon spectral amplitude has a phase (a frequency chirp) depending nonlinearly on the frequency and making the two-photon wavepackets not Fourier transform-limited. Therefore, in these examples the biphotons are not short in time despite their broad frequency spectrum. In Ref. [9] it was mentioned that time compression of such two-photon wavepackets requires compensation for their frequency chirp, although the way to eliminate the chirp was not specified. Recently we have demonstrated [15] that broadband biphoton wave packets produced via SPDC in APPC can be compressed in time by using group-velocity dispersion (GVD) in standard opti-

cal fiber. A Fourier limited compression was obtained in [15] via an analytical calculation within the approximation of large difference in the group velocities of the two SPDC photons and neglecting third-order GVD of the fiber. Furthermore, we have given an example of a complete numerical calculation demonstrating that higher orders do not change this result.

With the purpose of paving the way for a realistic experimental implementation of this idea and application to quantum technologies [16], here we present and discuss a systematic study of this phenomenon. Furthermore, we present some optimal situation where the full numerical calculation shows an effect that can be clearly observed with a realistic set-up.

II. SPECTRAL PROPERTIES OF BIPHOTONS EMITTED IN A MEDIUM WITH SECOND-ORDER SUSCEPTIBILITY VARYING ALONG THE PUMP PROPAGATION

Spontaneous Parametric Down Conversion occurs in non-linear dielectric crystals and consists of the spontaneous decay of a photon (pump) of frequency ω_p in two photons of lower frequencies ω_s and ω_i , historically named signal and idler, satisfying, in an ideal case, the constraints of energy and momentum conservation. In what follows we will consider type II collinear SPDC interaction, with the pump being a linearly (ordinarily) polarized monochromatic plane wave propagating along the z direction and the signal and idler fields being extraordinarily and ordinarily polarized, respectively. Considering signal and idler fields initially in the vacuum state, the output state is

$$|\psi\rangle = |0\rangle + \int d\omega_s d\omega_i F(\omega_s, \omega_i) \hat{a}_{\omega_s}^\dagger \hat{b}_{\omega_i}^\dagger |0\rangle, \quad (1)$$

where, due to the weak interaction, only the first two terms of the perturbative expansion are considered [17]. In Eq. (1), $\hat{a}_{\omega_s}^\dagger$ and $\hat{b}_{\omega_i}^\dagger$ are the photon creation operators for signal and idler photons, respectively.

The function $F(\omega_s, \omega_i)$ is the Two-Photon Spectral Amplitude (TPSA) and accounts, in particular, for the non-linearity of the crystal $\chi^{(2)}$ and the wavevector mismatch $k_p - k_s - k_i$. The second-order susceptibility is assumed to depend on the pump propagation direction z only; for cw pumping, the TPSA is

$$F(\omega_s, \omega_i) \propto \delta(\omega_p - \omega_s - \omega_i) \int_{-L}^0 dz \chi^{(2)}(z) e^{i(k_p - k_s - k_i)z}, \quad (2)$$

where L is the length of the crystal and the wavevectors $k_j = \frac{n_j(\omega_j)\omega_j}{c}$ ($j = p, s, i$) depend on the ordinary or extraordinary refractive indexes n_j of the crystal [18]. The TPSA determines all the spectral and temporal properties of two-photon light. In the general form, its square module gives the spectrum of the biphoton radiation. For example, the signal spectrum is

$$S(\omega_s) = \left| \int d\omega_i F(\omega_s, \omega_i) \right|^2, \quad (3)$$

and similarly for the idler spectrum.

In bulk crystals the momentum conservation is ensured, for each frequency, by choosing a proper direction of the waves involved in the process. Nevertheless, in type II SPDC the efficiency of the process is reduced by birefringence walk-off. The advantage of using poled crystals for biphoton generation relies on the absence of transverse walk-off and allows one to avoid using narrow-band filtering in certain experiments. Moreover, compared with a bulk crystal, a poled material provides a higher SPDC pair production efficiency due to noncritical quasi-phase matching (QPM), obtainable at a given temperature, or due to the possibility to utilize the largest value of the effective nonlinear coefficient.

According to [22], let us consider a square nonuniform first-order QPM grating with slow variation of the poling period $\Lambda(z)$. Then the spatial variation of the second-order susceptibility along the medium can be written as

$$\chi^{(2)}(z) = \chi_0^{(2)} e^{iK_0 z + i\Phi_0(z)}, \quad (4)$$

where the absolute value of the second-order susceptibility is constant. The phase $\Phi_0(z)$ in Eq. (4) is induced by the modulation of the local wavevector $\kappa(z) = 2\pi/\Lambda(z)$. The wavevector varies linearly within the length of the crystal (linearly chirped QPM grating), thus [22]

$$\kappa(z) = K_0 + \frac{d\Phi_0(z)}{dz} = K_0 - 2\alpha(z + \frac{L}{2}), \quad (5)$$

where α is defined as the chirping parameter and K_0 is chosen so that perfect collinear first-order quasi phase matching for selected frequencies ω_{s0} and $\omega_{i0} = \omega_p - \omega_{s0}$ is obtained at the center of the crystal, i.e.,

$$k_p(\omega_p) - k_s(\omega_{s0}) - k_i(\omega_p - \omega_{s0}) - K_0 = 0. \quad (6)$$

The phase of the grating, obtained by integrating Eq. (5) (except for an unessential constant phase factor), is

$$\Phi_0(z) = -\alpha(z + \frac{L}{2})^2 \quad (7)$$

and it equals zero at the center of the crystal.

The TPSA gains a phase shift that depends nonlinearly on the frequency because of the presence of this phase factor in the second-order nonlinear coefficient. In fact, doing analytically the integral in Eq. (2), we find that the TPSA takes the form

$$F(\omega_s, \omega_i) \propto e^{i\phi(\omega_s, \omega_i)} \times \left(\frac{\text{Erf}[\frac{(-1)^{1/4}(L\alpha - \Delta k)}{2\sqrt{\alpha}}]}{\sqrt{\alpha}} + \frac{\text{Erf}[\frac{(-1)^{1/4}(L\alpha + \Delta k)}{2\sqrt{\alpha}}]}{\sqrt{\alpha}} \right) \times \delta(\omega_p - \omega_s - \omega_i) \quad (8)$$

where Erf is the error function and $\Delta k(\omega_s, \omega_i) = k_p - k_s - k_i - K_0$. The phase factor shows a nonlinear dependence on $\Delta k(\omega_s, \omega_i)$:

$$\phi(\omega_s, \omega_i) = \frac{\Delta k(\omega_s, \omega_i)L}{2} + \frac{\Delta k^2(\omega_s, \omega_i)}{4\alpha}. \quad (9)$$

As a consequence, the phase depends nonlinearly on the frequency, as discussed in more detail in section III. This phase factor does not affect the spectrum of the biphoton wavepackets as it is evident from (3). Nevertheless, it is of huge importance when considering the temporal behavior of the wavepacket [9]. On the contrary, the error function in Eq. (8) affects the width of the spectrum of biphotons and the effect is the broadening of the spectrum when increasing the aperiodicity.

III. TEMPORAL PROPERTIES

In Fig. 1 a typical experimental set-up for the measurement of the time separation between the arrivals of the two photons, τ , is depicted. Photons of a pair produced by type II SPDC are orthogonally polarized, and can be easily separated by a polarizing beam-splitter and addressed to two different photon counting detectors, D1 and D2.

The rate of coincidences between signal and idler photons reaching detectors at times t' and t'' , respectively, can be expressed as [13]

$$R_c \propto \iint dt' dt'' G_{meas}^{(2)}(t'; t'') \Pi(t' - t'', T_W), \quad (10)$$

where $\Pi(t' - t'', T_W)$ is the rectangular coincidence window function of temporal width T_W and $G_{meas}^{(2)}(t'; t'')$ is the second-order Glauber's correlation function, where, for convenience, not only the electric field operators are

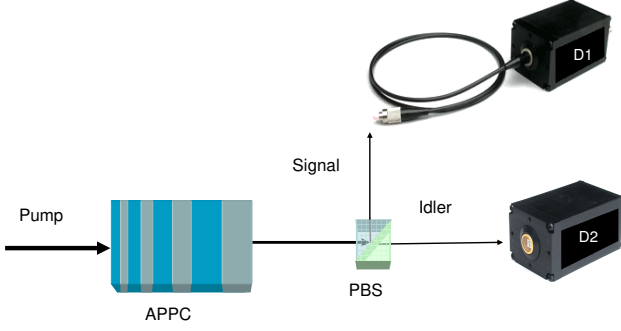


FIG. 1: (color online) A typical set-up for observing two-photon coincidences in type-II SPDC. A laser beam pumps a type-II aperiodically poled crystal (APPC) in collinear regime. After a polarizing beam splitter (PBS), signal and idler beams are addressed to low-jitter photodetectors, whose outputs are sent to a coincidence circuit.

incorporated, but also the spectral response functions of the signal and idler detection arms, f_s and f_i , respectively. $G_{meas}^{(2)}(t'; t'')$ stands then for the measured value of Glauber's correlation function. Then,

$$\begin{aligned} G_{meas}^{(2)}(t'; t'') &= \langle \psi | \hat{A}_s^\dagger(t') \hat{B}_i^\dagger(t'') \hat{B}_i(t'') \hat{A}_s(t') | \psi \rangle \\ &= \| \langle 0 | \hat{B}_i(t'') \hat{A}_s(t') | \psi \rangle \|^2, \end{aligned} \quad (11)$$

where

$$\begin{aligned} \hat{A}_s(t') &= \int d\omega_s f_s(\omega_s) e^{-i\omega_s t'} \hat{a}_{\omega_s}, \\ \hat{B}_i(t'') &= \int d\omega_i f_i(\omega_i) e^{-i\omega_i t''} \hat{b}_{\omega_i}. \end{aligned}$$

Typically in the literature (see for example Ref. [17]) there is no spectral dependence of the detection arms, and the operators $A_s(t')$ and $B_s(t'')$ are usual quantized electric fields, i.e.,

$$f_x(\omega_x) \propto 1, \quad (12)$$

with $x = s, i$. However, in the general case the spectral response of the detection channel should be taken into account since it influences both spectral and temporal properties of the measured two-photon wavepackets. For instance, considering Gaussian spectral responses of the detection channels, we have

$$f_x(\omega_x) \propto e^{-\frac{(\omega_x - \omega_{xc})^2}{(\delta\omega)^2}}, \quad (13)$$

where ω_{xc} is the selected central frequency of the spectral response and $\delta\omega$ is its width. According to Ref. [23],

the measured time two-photon amplitude (TTPA) is expressed as

$$\begin{aligned} \langle 0 | B_i(t'') A_s(t') | \psi \rangle &= \int d\omega_s d\omega_i F(\omega_s, \omega_i) f_s(\omega_s) f_i(\omega_i) \\ &\quad \times e^{-i\omega_s t'} e^{-i\omega_i t''}. \end{aligned} \quad (14)$$

The measured spectrum (3) of the wavepacket is also modified by the detection arms spectral filtering as

$$S(\omega_s) = \left| \int d\omega_i F(\omega_s, \omega_i) f_s(\omega_s) f_i(\omega_i) \right|^2. \quad (15)$$

Until the end of the next section we will consider only the simplest case of detection arms without any spectral dependence, i.e., $f_x(\omega_x) = 1$, in order to focus on the temporal properties of the emission. The discussion on the modification of the temporal properties induced by the spectral characteristics of the detection arms is postponed to section V. To discuss the difference in the arrival times of the signal photon, t' , and the idler one, t'' , on the detectors, we introduce the new variables:

$$\begin{aligned} \tau &= t' - t'' \\ T &= t' + t''. \end{aligned} \quad (16)$$

Thus, the TTPA can be rewritten as the Fourier transform of the TPSA:

$$\begin{aligned} F(\tau) &= \langle 0 | B_i(t'') A_s(t') | \psi \rangle \\ &\propto \int d\omega_s F(\omega_s, \omega_p - \omega_s) e^{i\omega_s \tau}. \end{aligned}$$

The square module of the TTPA is the measured Glauber's second-order correlation function,

$$G_{meas}^{(2)}(\tau) = |F(\tau)|^2 \quad (17)$$

and the width of $G_{meas}^{(2)}(\tau)$ will be further referred to as correlation time.

IV. TEMPORAL BIPHOTON COMPRESSION

Since the TTPA is the Fourier transform of TPSA, a necessary condition for reaching ultra narrow correlation time is producing ultra broadband SPDC light. In the case of aperiodically poled crystals with linear chirping, the phase factor depending nonlinearly on z is responsible for the spectral broadening effect and increasing the aperiodicity broadens the spectrum. Unfortunately, the two-photon spectral amplitude is not Fourier transform limited because of the presence of the phase factor (9) in Eq. (8).

Thus, the spread in the detection time difference of the two photons cannot be reduced simply by broadening the spectrum. As suggested in Ref. [9], the ideal way to make TTPA perfectly Fourier transform limited is to insert in

the path of the biphotons a proper optical medium that compensates for the nonlinear part of the phase factor in Eq. (9). In general the insertion of an optical medium with refractive index $n_{mx}(\omega)$ and of length l_x in both optical paths $x = s, i$ adds to the TPSA the phase factor $e^{i(k_{ms}(\omega_s)l_s + k_{mi}(\omega_i)l_i)}$, where $k_{mx} = \frac{n_{mx}(\omega_x)\omega_x}{c}$. Denoting the TPSA after the propagation of biphotons through the optical medium as F_m , we have

$$F_m(\omega_s, \omega_i) = e^{i(k_{ms}(\omega_s)l_s + k_{mi}(\omega_i)l_i)} F(\omega_s, \omega_i). \quad (18)$$

In Ref. [9] it was shown that a correlation time at the Fourier transform limit can be achieved when the inserted optical media satisfies the condition

$$k_{ms}(\omega_s)l_s + k_{mi}(\omega_p - \omega_s)l_i = -\phi(\omega_s, \omega_p - \omega_s). \quad (19)$$

In Ref. [15] it was shown that, in some specific cases, this can be achieved by passing one of the two photon through a normal-dispersion medium, for example a standard optical fiber. This result opens a perspective of a real implementation of the method suggested in Ref. [9]. In particular, we considered the simplest case where in Eq. (19) the terms of orders higher than two in the frequency expansion of the wavevector are negligible. Here we explicitly discuss the effect of considering such higher-order terms in the frequency expansion of Eq. (19). The first obvious consideration is that a perfect Fourier transform limited compression does not require Eq. (19) to be satisfied; in fact, it is sufficient to satisfy its second-order derivative:

$$\frac{d^2}{d\omega_s^2} [k_{ms}(\omega_s)l_s + k_{mi}(\omega_p - \omega_s)l_i] = -\frac{d^2}{d\omega_s^2} \phi(\omega_s, \omega_p - \omega_s). \quad (20)$$

Furthermore, it is worth observing that Eq.(20) should be satisfied only for the values of ω_s where the TPSA is nonzero.

In order to understand how to satisfy, at least approximately, the condition in Eq. (20) we compare the behavior of the second-order derivative of the Harris Phase factor, $-\frac{d^2}{d\omega_s^2} \phi(\omega_s, \omega_p - \omega_s)$ (HP), which needs to be eliminated to provide the temporal compression of the biphoton at the Fourier limit, and the one induced by the presence of the optical fibers of appropriate lengths in the signal and idler channels, $\frac{d^2}{d\omega_s^2} [k_{ms}(\omega_s)l_s + k_{mi}(\omega_p - \omega_s)l_i]$ (OFP). We considered collinear type II, almost degenerate, SPDC emission in an aperiodically poled KTP crystal (APKTP). The monochromatic pump at 458 nm and the idler field are ordinarily polarized, while the signal field is extraordinarily polarized. The dependence of wavevectors on the frequency in KTP is evaluated exploiting Sellmeier equations [24] and we consider the first-order QPM. The phase mismatch at the center of the APKTP crystal is compensated for by the inverse grating vector $K_0 = 2441.8 \text{ cm}^{-1}$, corresponding to degenerate emission at 916 nm. Spectral and temporal properties of the SPDC radiation, as well as the temporal compression

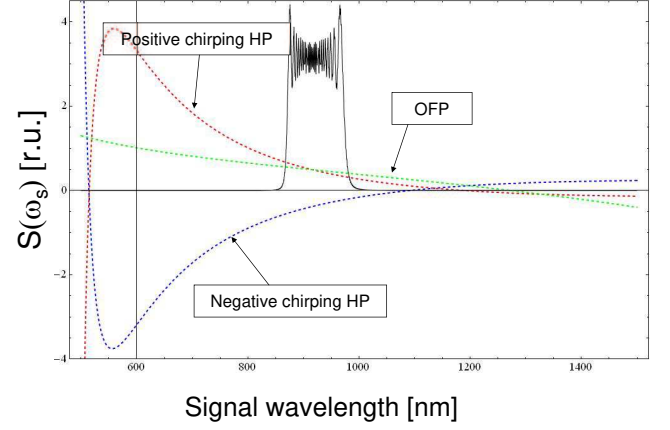


FIG. 2: (color online) The dependence of HP and OFP on the signal wavelength (both for positive and negative chirping) with the optical fiber present only in the signal channel, for a crystal with $L = 0.8 \text{ cm}$ and $|\alpha| = 50 \text{ cm}^{-2}$. For completeness, the spectrum of the biphoton field is shown as well

of the biphoton wavepackets in the optical fiber, are numerically calculated for several different parameters such as the length of the crystal, the chirping parameter and the fiber length. No frequency expansion of the wavevector is involved, in contrast to Ref. [15] where the analysis was performed analytically and only up to second-order terms in frequency.

Fig. (2) shows the dependence of HP and OFP on the signal wavelength in the case where the optical fiber is present only in the signal channel, for a crystal with $L = 0.8 \text{ cm}$ and $|\alpha| = 50 \text{ cm}^{-2}$. For completeness, the spectrum of the biphoton field is shown as well. It is interesting that the effect of the optical fiber in either signal or idler SPDC channel is different for the cases of positive ($\alpha > 0$) and negative ($\alpha < 0$) chirping parameter. In fact, since temporal compression is achieved due to the group velocity dispersion in a standard optical fiber, only in the case of negative chirping the HP can be approximately compensated by the OFP. Temporal compression in the case of $\alpha > 0$ can be obtained only in a specially engineered fiber with negative group velocity dispersion, whose study is beyond the scope of this paper.

The maximum value of the compression is achieved for the length of the fiber l_f providing the best agreement between the HP and OFP, approximately corresponding to the situation where HP and OFP have the same value at the degenerate wavelength (916 nm), as shown in Fig. 2. The dependence of the correlation time on the optical fiber length is shown in Fig. 3 both for positive and negative chirping parameter. The effect of the optical fiber in the first case is an increase in the correlation time, i.e., broadening of $G_{meas}^{(2)}(\tau)$, while in the second case the insertion of the fiber leads to a compression of

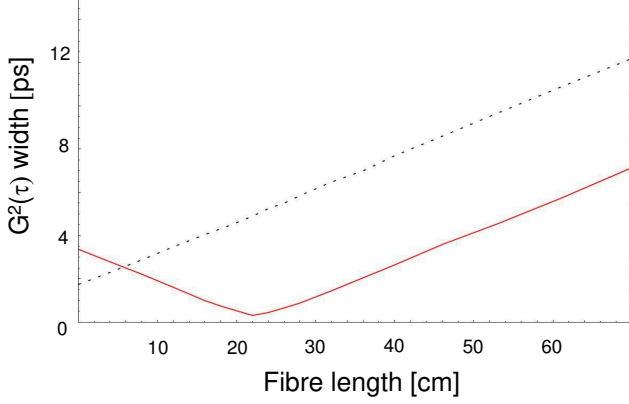


FIG. 3: (color online) Dependence of the correlation time on the optical fiber length. The two lines refer to positive (dashed line) and negative (solid line) chirping parameters.

$G_{meas}^{(2)}(\tau)$, until its minimum width is reached at $l = l_f$. The compression is then followed by a broadening of $G_{meas}^{(2)}(\tau)$.

At $l = 0$ the computed correlation times do not have the same values for negative and positive chirp. This effect is due to the generation of signal and idler photons at different frequencies at the beginning and at the end of the crystal. In fact, biphotons are degenerate only at the center of the crystal and the frequency difference causes distinct delays between the two photons. During the propagation of biphotons in the crystal, the delay due to the frequency difference is compensated by the e-o delay in the case of $\alpha > 0$ but in the case of $\alpha < 0$, the delays add up.

In [15] it was shown that within the second-order frequency series expansion of $\phi(\omega_s, \omega_p - \omega_s)$, perfect temporal compression of $G_{meas}^{(2)}(\tau)$ can be achieved with normal dispersive media. Let us now discuss the effect of higher-order terms in the expansion on the width of the compressed $G_{meas}^{(2)}(\tau)$. Fig. 4 reports the results obtained via exact numerical calculation for a crystal with $L = 0.8$ cm and $|\alpha| = 20$ cm⁻². The left-hand part of the figure shows the shape of $G_{meas}^{(2)}(\tau)$ at the output of the crystal, with no dispersive medium inserted, while the right-hand part illustrates the effect of a 1.06 m long fiber inserted into the SPDC signal channel. The a) and b) parts refer to a crystal with $\alpha < 0$ while the c) and d) parts, to an $\alpha > 0$ crystal. In the case of negative chirping, the compressed $G_{meas}^{(2)}(\tau)$ takes almost the shape of an ideal sinc function, meaning that time compression at the Fourier limit is almost achieved [15]. The estimated FWHM of $G_{meas}^{(2)}(\tau)$ is reduced from 2.8 ps to 67 fs (which is the value at the Fourier limit), as it is clear from Fig. 5, where the spectrum of the corre-

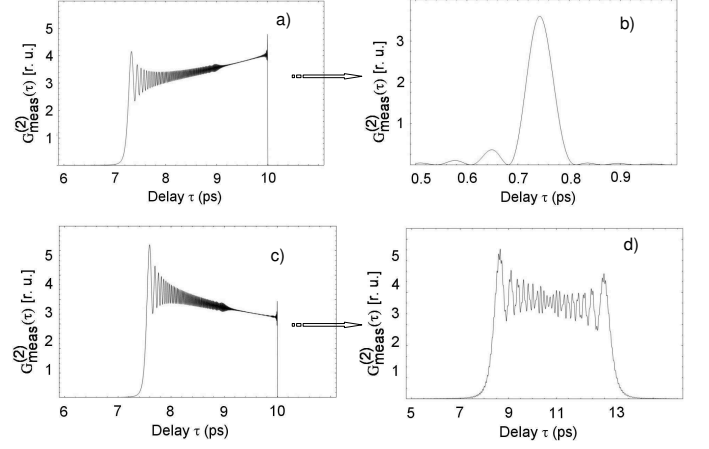


FIG. 4: (color online) $G_{meas}^{(2)}(\tau)$ evaluated via exact numerical calculation for a crystal with $L = 0.8$ cm and $|\alpha| = 20$ cm⁻². The left-hand part of the figure shows the shape of $G_{meas}^{(2)}(\tau)$ at the output of the crystal, with no dispersive medium inserted, while the right-hand part illustrates the effect of a 1.06 m long fiber inserted into the SPDC signal channel. The a) and b) parts refer to a crystal with $\alpha < 0$ while the c) and d) parts, to an $\alpha > 0$ crystal.

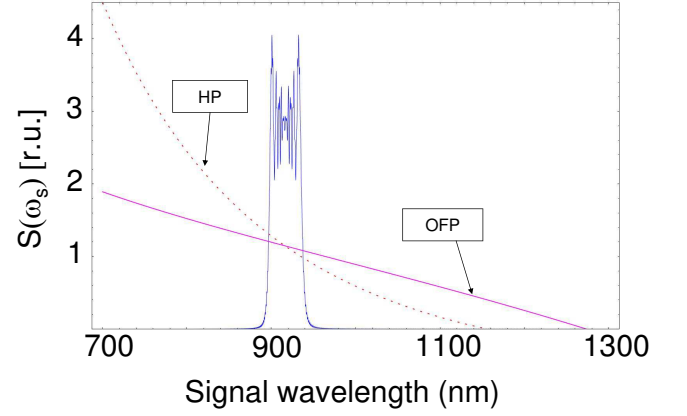


FIG. 5: (color online) The spectrum of biphotons, with the width of approximately 40 nm, as well as HP and OFP frequency dependencies (dashed and solid lines, respectively).

sponding biphoton wavepacket is shown. Summarizing, Fig. 4 shows that a normal dispersive medium, as an optical fiber, can compress the biphoton wavepacket to the Fourier limit. The effect is opposite in the case of $\alpha > 0$: the initial correlation time of 2.6 ps is increased to become 5 ps.

With this choice of crystal parameters, the condition given by Eq.(20) should be satisfied in a quite narrow region of nonzero signal field spectrum. Fig. 5 shows

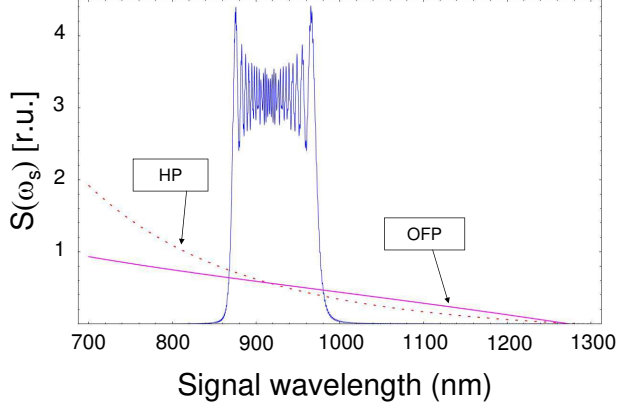


FIG. 6: (color online) The spectrum of biphotons as well as HP and OFP frequency dependencies (dashed and solid lines, respectively), for a crystal with $L = 1.8$ cm and $\alpha = -50$ cm^{-2}

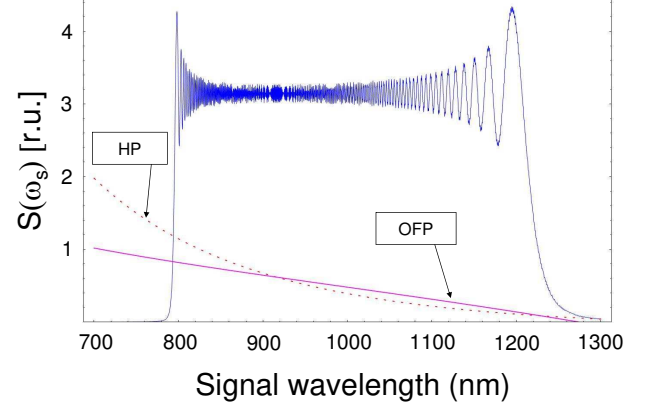


FIG. 8: (color online) The spectrum of biphotons as well as HP and OFP frequency dependencies (dashed and solid lines, respectively), for a crystal with $L = 2.5$ cm and $\alpha = -50$ cm^{-2}

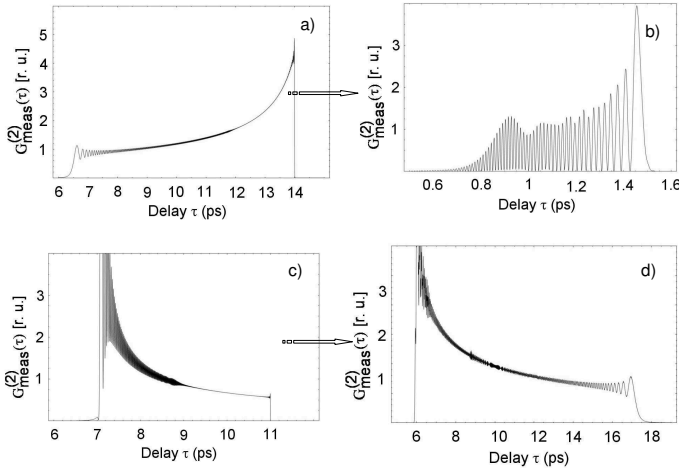


FIG. 7: (color online) Effect of inserting a 0.52 m long fiber (right-hand side) on the correlation time for the case shown in Fig. (6)

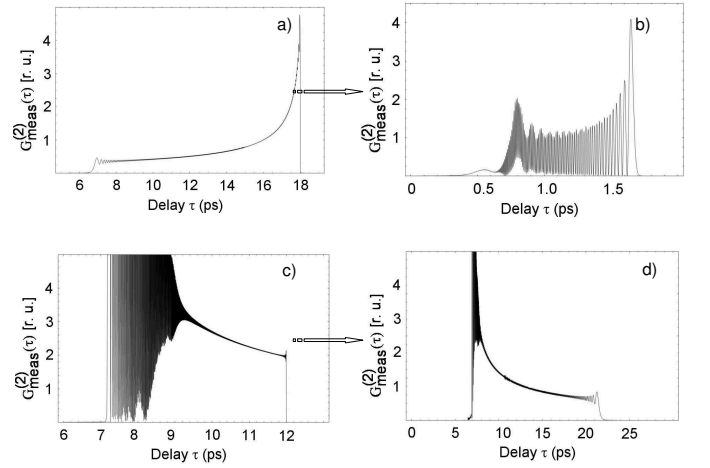


FIG. 9: (color online) Effect of inserting a 0.57 m long fiber (right-hand side) on the correlation time for the case shown in Fig. 8

the spectrum of biphotons, approximately 40 nm wide, as well as HP and OFP lines: their superimposition, in the case of negative chirping, is easily obtained in such a narrow spectral region. However, an increase in either the length of the crystal or the chirping parameter leads to a broadening of the spectrum.

Figs. 6 and 8 are analogues of Fig. 5 for two different crystals. In both cases, the same chirping parameter $\alpha = -50$ cm^{-2} is considered while the length is $L = 1.8$ cm in the first case and $L = 2.5$ cm in the second one. As the crystal length is increased, the spectrum becomes broader and broader, its width growing from 300 nm in

the first case to 500 nm in the second one. As a consequence, the HP and OFP frequency dependencies must be superimposed in a larger region, and, as in general this cannot be achieved, the perfect temporal compression of the $G_{meas}^{(2)}(\tau)$ is slightly deteriorated.

The compressed peaks become more noisy and start to differ from the sinc function and, as a consequence, the width is slightly increased. Figs. 7 and 9 show the effect of the insertion of the fiber. The length of the fiber is 0.52 m in the first case and 0.57 m in the second case. However, a significant compression still remains: from 7.5 ps to 700 fs in the first case and from 11.25 ps to 1 ps in

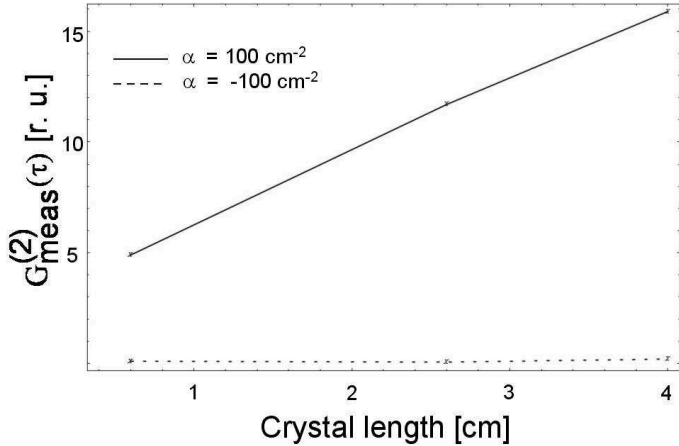


FIG. 10: (color online) Correlation time as a function of the length L of the crystal with the chirping parameter $\alpha = 100\text{cm}^{-2}$ (solid line) and $\alpha = -100\text{cm}^{-2}$ (dashed line).

the second case. The correlation time is reduced in both cases by about an order of magnitude, confirming that ultrabroadband PDC light can be generated in chirped crystals and that temporal compression can be achieved in a standard optical fiber.

Fig. 10 shows the correlation time as a function of the length L of a crystal with the chirping parameter $\alpha = 100\text{cm}^{-2}$ (solid line) and $\alpha = -100\text{cm}^{-2}$ (dashed line). Each point refers to the value that the correlation time takes after the passage of the signal photon through a fiber with the length optimized for the maximum compression in the case of negative-chirped crystals. The plot demonstrates that the difference between the correlation times for positive and negative chirping parameters becomes more pronounced for longer crystals. In fact, an increase in the crystal length leads to a growth of the correlation time in the case of $\alpha > 0$. Calculation shows that for $\alpha < 0$, an increase in L affects the correlation time very little, although a perfect compression would result in the correlation time inversely proportional to L . In any case, the width of compressed $G_{meas}^{(2)}(\tau)$ is always below 200 fs, at least for the range of crystal length considered.

It is interesting to point out that the curves in Fig. 10 are not affected by changing the absolute value of the chirping parameter. We have computed the correlation times for both positive and negative α with the absolute value varying in the range $20 - 500\text{cm}^{-2}$, for three lengths of the crystal (0.8 cm, 1.8 cm and 2.5 cm) and no significant difference was observed. This seems very promising for the temporal compression of ultra-broadband biphotons, as increasing the chirping parameter leads to a broadening of the spectrum, as shown in Fig. 11. For example, for a crystal of $L = 2.5\text{ cm}$, if the absolute value of the chirping parameter is increased from 50 cm^{-2} to 500 cm^{-2} the corresponding spectrum

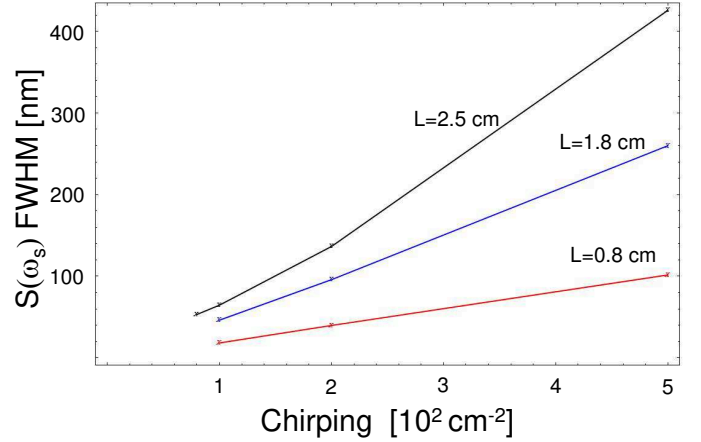


FIG. 11: (color online) Correlation time as a function of the chirping parameter, for three different crystal lengths.

width will change from 53.28 nm to 425.86 nm and, at the same time, the correlation time of the compressed biphoton wavepacket can be still below 1 ps simply with a standard fiber in the signal channel.

Furthermore, we found that the length of the fiber to be inserted for the temporal compression is almost independent of the crystal length. At the same time, it is reduced with the increase of α , passing from 2 m to 50 cm approximately in the range of the chirping parameters considered above.

V. SPECTRAL FILTERING EFFECTS

In the previous section we considered the spectral and temporal properties assuming the absence of spectral selection in the detection arms. Here, we discuss how the presence of such spectral selection associated with the detection process modifies the measured spectral and temporal properties of the biphoton wavepacket as well as the measurement of its temporal compression. In particular, we consider detection arms with Gaussian spectral filtering as the one in Eq. (13) centered at 532 nm ($\omega_{sc} = \omega_{ic} = 3222\text{ THz}$) and width 250 nm ($\delta\omega = 716\text{ THz}$). Fig. 12 presents the effective spectral behavior of such detection arms for signal/idler wavelengths in the region of interest, and it is in agreement with the typical spectral response of certain commercial single-photon detectors.

For comparison, we analyze the case of two APKTP crystals already considered in the previous section. The first one has the chirping parameter $\alpha = -20\text{ cm}^{-2}$ and length $L = 0.8\text{ cm}$. The spectrum not accounting for detection spectral filtering is shown in Fig. 5, and the corresponding temporal behavior is shown in Fig. 4. The second one has parameters $\alpha = -50\text{ cm}^{-2}$ and $L = 2.5\text{ cm}$, and its spectral and temporal behavior (with no ac-

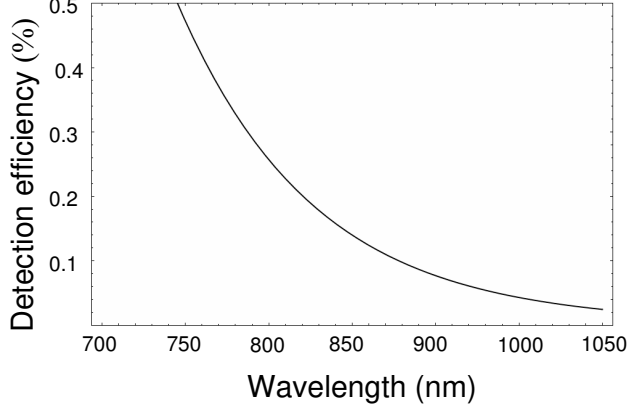


FIG. 12: (color online) Simulated spectral response of a single-photon detector.

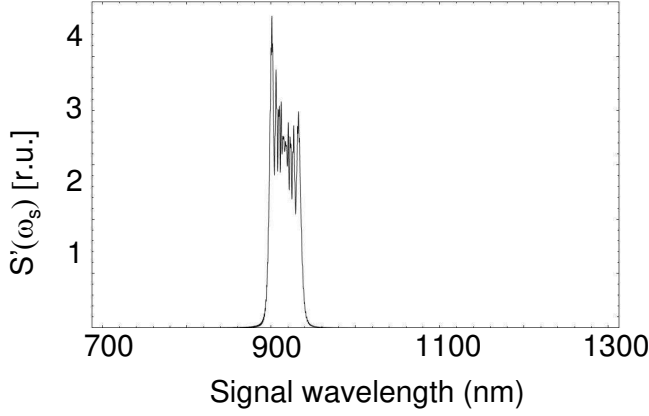


FIG. 13: (color online) The modified spectrum of biphotons for a crystal with $L = 0.8$ cm and $\alpha = -20$ cm⁻².

count for the detection spectral filtering) is shown in Fig. 8 and Fig. 9, respectively. Figs. 13 and 15 show the spectrum of the biphoton wavepackets modified by the detection spectral filtering of Fig. 12 in the case of the first and the second crystals, respectively.

As the spectrum in Fig. 13 is quite narrow and its shape is not modified much with respect to the one in Fig. 5, it is reasonable to expect that also the corresponding $G_{meas}^{(2)}(\tau)$, both with and without the fiber for temporal compression, is not modified much by the presence of the detection spectral filtering. This is confirmed by the comparison between Fig. 14 and Fig. 4.

On the contrary, the wide spectrum of Fig. 8 is strongly distorted by the presence of the detection spectral filtering as shown in Fig. 15. The temporal counterpart of this distortion can be found in Fig. 16 where

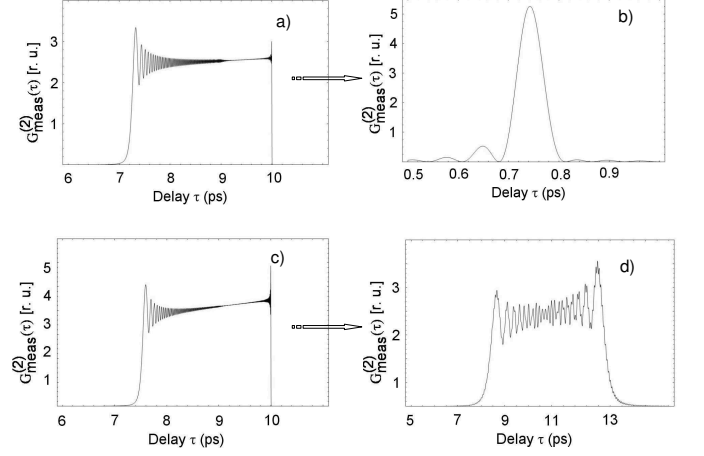


FIG. 14: (color online) Effect of a 1.06 m long fiber inserted into the signal channel (right hand side) on $G_{meas}^{(2)}(\tau)$ for the case shown in Fig. 13

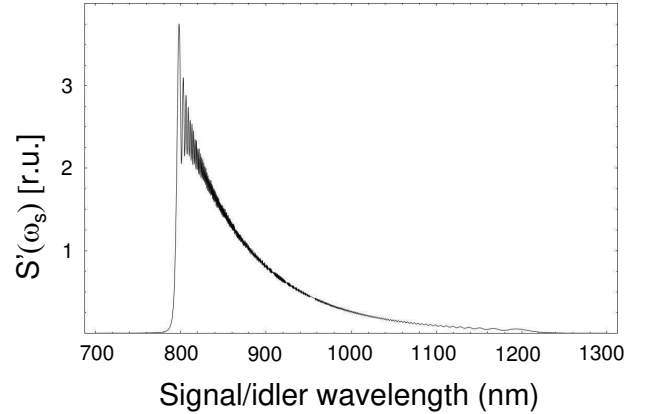


FIG. 15: (color online) The modified spectrum of biphotons for a crystal with $L = 2.5$ cm and $\alpha = -50$ cm⁻².

$G_{meas}^{(2)}(\tau)$ manifests shapes modified with respect to the ones in Fig. 9, even if the correlation time widths look not so different.

Summarizing, the spectral filtering in the detection arms affects not only the measured spectral properties of the biphoton wavepacket, but also its measured temporal properties. Thus, to achieve temporal compression with ultrabroadband PDC light, one has to take care of the spectral filtering of the detection systems for its effect on both spectral and temporal behavior of biphoton wavepackets.

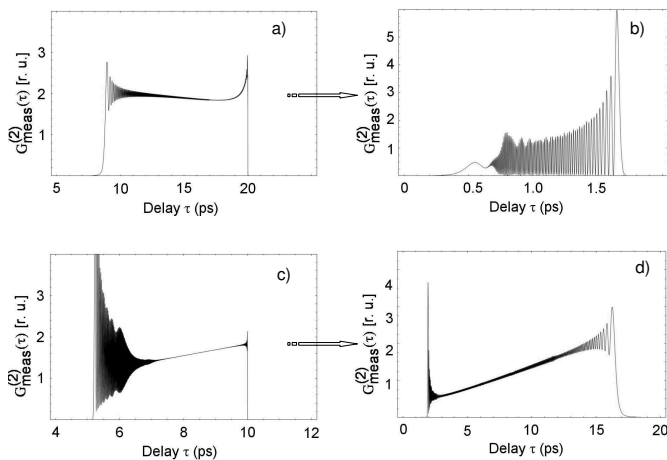


FIG. 16: (color online) Effect of inserting a 0.57 m long fiber (right-hand side) on $G_{meas}^{(2)}(\tau)$ for the case shown in Fig. 15

VI. CONCLUSION

Producing nonclassical light with tailored spectral and temporal properties represents a fundamental resource for developing quantum technologies, such as quantum lithography, quantum metrology, two-photon coherent absorption, etc. Aiming at an effective practical realization of our ideas, first presented in [15], in this paper we have systematically discussed the possibility of generating two-photon wavepackets with correlation times as small as possible by exploiting aperiodically poled crystals together with standard optical fibers. The analysis carried out here is numerical, taking into account the exact dispersion dependencies in the crystal and the fiber, given by the Sellmeier equations. This is a considerable step forward compared to the previous work where the effect was mainly described analytically, but only in the framework of the second-order approximation in the frequency expansion of the phase mismatch. From our numerical calculations it follows that higher-order terms

in the frequency expansion of the wavevector mismatch, as well as in the fibre dispersion dependence, considerably change the shape of the compressed two-photon wavepacket. However, the effect of compression is still present. The dependence of this effect on the crystal length and the chirping parameter has been analyzed. Our results clearly show that a significant compression, i.e. reduction of correlation times by more than one order of magnitude, can be easily reached, achieving correlation times as short as hundreds of femtoseconds. In our analysis we also discussed the effect of possible spectral filtering in detection arms. Despite spectral filtering modifies the correlation time of the biphoton wavepacket as well as its spectrum, it is noteworthy to observe that, at least in the case considered, the temporal compression is essentially preserved. Direct experimental observation of such a compression by means of coincidence measurement is possible only if the detectors' jitter is smaller than the correlation time of the biphoton wavepacket. Even if hundreds of femtoseconds jitter seems hardly achievable for present days detector technologies, it could be a target of next future detectors [25–28]. Furthermore, undirect measurements can be envisaged [29]. Since our scheme only requires relatively simple and available technologies (i.e. chirped poled crystals and commercial optical fibers), we have demonstrated the feasibility of a suitable practical realization of ultracompressed biphotons.

Acknowledgments

This work has been supported in part by MIUR (PRIN 2007FYETBY), "San Paolo foundation", NATO (CBP.NR.NRCL 983251), RFBR 08-02-00555a, Russian Federal Agency for Science and Innovation (Rosnauka) state contract 02.740.11.0223, and the Russian Program for Scientific Schools Support, grant # NSh-796.2008.2. M. V. Ch. also acknowledges the support of the CRT Foundation.

-
- [1] B. Dayan, A. Pe'er, A. A. Friesem, and Y. Silberberg, Phys. Rev. Lett., **93**, 023005 (2004).
 - [2] B. Dayan, Phys. Rev. A **76**, 043813 (2007).
 - [3] J. Gea-Banacloche, Phys. Rev. Lett. **62**, 1603 (1989).
 - [4] N. Ph. Georgiades, E. S. Polzik, K. Edamatsu, H. J. Kimble, and A. S. Parkins, Phys. Rev. Lett. **75**, 3426 (1995).
 - [5] B. Dayan, A. Peér, A. A. Friesem, and Y. Silberberg, Phys. Rev. Lett. **94**, 043602 (2005).
 - [6] A. Valencia, G. Scarcelli, and Y. Shih, Appl. Phys. Lett., **85**, 13 (2004).
 - [7] A. Valencia, A. Cere, X. Shi, G. Molina-Terriza, and J. P. Torres, Phys. Rev. Lett. **99**, 243601 (2007).
 - [8] S. Carrasco, M. B. Nasr, A. V. Sergienko, B. E. A. Saleh, and M. C. Teich, Optics Letters **31**, 253 (2004).
 - [9] S. E. Harris, Phys. Rev. Lett. **98**, 063602 (2007).
 - [10] M. B. Nasr, S. Carrasco, B. E. A. Saleh, A. V. Sergienko, M. C. Teich, J. P. Torres, L. Torner, D. S. Hum, and M. M. Fejer, Phys. Rev. Lett. **100**, 183601 (2008).
 - [11] D. A. Kalashnikov, K. G. Katamadze, and S. P. Kulik, JETP, **89**, 264 (2009).
 - [12] M. V. Chekhova, JETP Lett., **75**, 225-226 (2002).
 - [13] A. Valencia, M. V. Chekhova, A. S. Trifonov and Y. H. Shih, Phys. Rev. Lett. **88**, 183601 (2002).
 - [14] D. Strekalov, A. B. Matsko, A. A. Savchenkov, and L. Maleki, Phys. Rev. A **71**, 041803(R) (2005).
 - [15] G. Brida, M. V. Chekhova, I. P. Degiovanni, M. Genovese, G. Kh. Kitaeva, A. Meda, and O. A. Shumilkina, Phys. Rev. Lett. **103**, 193602 (2009).

- [16] M. Genovese, Phys. Rep. **413**, 319 (2005).
- [17] L. Mandel, and E. Wolf, *Optical Coherence and Quantum Optics*, (Cambridge University Press, Cambridge, 1995).
- [18] D. N. Klyshko, Sov. Phys. JETP Lett. **6**, 85 (1967).
- [19] D. C. Burnham, D.L. Weinberg, Phys.Rev.Lett., **25**, 84 (1970).
- [20] J. A. Armstrong, N. Bloembergen, and P. S. Pershan, Phys. Rev. **127**, 1918 (1962).
- [21] M. M. Fejer, G. A. Magel, D. H. Jundt, and R. L. Byer, IEEE J. Quantum Electron **28**, 11 (1992).
- [22] G. Imeshev, M. A. Arbore, M. M. Fejer, A. Galvanauskas, M. Fermann, and D. Harter, J. Opt. Soc. Am. B **17**, 304 (2000).
- [23] T. E. Keller, and M. H. Rubin, Phys. Rev. A **56**, 1534 (1997).
- [24] V. Dmitriev , G. Gurzadyan, D. Nikogosyan, and G. Gurzadian, *Handbook of Nonlinear Optical Crystals* (Springer Verlag, Berlin, 1991).
- [25] R. J. Collins, R. H. Hadfield, V. Fernandez, S. W. Nam, and G. S. Buller, IEEE Electron. Lett. **43**, 3 (2007).
- [26] R. T. Thew, S. Tanzilli, L. Krainer, S. C. Zeller, A. Rochas, I. Rech, S. Cova, H. Zbinden, and N. Gisin, New J. Phys. **8**, 32 (2006).
- [27] A. Tosi, A. Dalla Mora, F. Zappa, S. Cova, J. Mod. Optic **56**, 2-3 (2009).
- [28] Introduction to the issue on single photon counting: Detectors and applications Author(s): M. A. Itzler, S. Cova, M. Wahl, A. Tomita, IEEE J. Sel. Top. Quant. **13**, 4 (2007).
- [29] Experimental work in progress.